sustainability

MDPI

Article

Fragile or Robust: Research on the Structure, Energy Flow, and Associated Environmental Factors of Nearshore Coral Reef Ecosystems in Hainan

Jianfeng Gan [1,2], Kaibiao Chen [1,3,4], Jinghuai Zhang [1,3,4], Xinming Lei [5], Lang Lin [6], Xin Hu [7], Guowei Zhou [5], Danping Xie [2] and Peng Xu [1,2,5,*]

[1] Nansha Island Coral Reef Ecosystem National Observation Research Station, Guangzhou 510300, China; ganjianfeng@scies.org (J.G.)
[2] South China Institute of Environmental Sciences, Ministry of Ecology and Environment, Guangzhou 510091, China
[3] South China Sea Environmental Monitoring Center, State Oceanic Administration, Guangzhou 510230, China
[4] Key Laboratory of Marine Environmental Survey Technology and Application, Ministry of Natural Resources, Guangzhou 511458, China
[5] CAS Key Laboratory of Tropical Marine Bio-Resources and Ecology, South China Sea Institute of Oceanology, Chinese Academy of Sciences, Guangzhou 510070, China
[6] South China Sea Area and Island Center, Ministry of Natural Resources (South China Sea Standard Measurement and Information Center, Ministry of Natural Resources), Guangzhou 510300, China
[7] Guangdong Center for Marine Development Research, Guangzhou 511458, China
* Correspondence: xupengjxhedu@163.com

Abstract

Coral reefs are typical ecosystems of high diversity and productivity, but they are facing significant degradation in their structure and function due to the dual stresses of climate change and human activities. To uncover the trophic structure, energy flow, and environmental driving mechanisms of nearshore coral reefs in Hainan, this study constructed mass balance models for five regions, Sanya, Changjiang, Lingao, Wenchang, and Wanning, using Ecopath with Ecosim, and conducted quantitative analysis in conjunction with satellite environmental monitoring data. The results showed that the trophic levels of functional groups in different ecosystems ranged from 1.00 to 5.00, with Sanya and Changjiang having the highest trophic levels (4.505, 4.656), higher than Lingao, Wenchang, and Wanning (3.776–3.924). The system average trophic transfer efficiency ranged from 15.98% to 30.25%, generally higher than the classic Lindeman 10% rule, with Changjiang being the highest (30.25%) and Lingao the lowest (15.98%). In terms of material cycling, the energy utilization efficiency of primary trophic levels was low, with a large amount of energy retained as detritus at lower trophic levels; Sanya and Changjiang showed more complete detritus chain energy cycling, with Finn cycling indices reaching 7.69 and 2.53, respectively, indicating higher maturity. Keystone analysis identified zooplankton, corals, and medium carnivorous fish as key functional groups with a decisive impact on system stability. Environmental correlation analysis revealed that particulate inorganic carbon (Pic), light diffuse attenuation coefficient (Kd), chlorophyll-a concentration (Chl_a), and sea surface temperature (Sst) were the main regulating factors, among which Pic showed a significant peaked relationship with the total system throughput, total biomass, and total production, with an optimal range of 0.0050–0.0075 mol/m^2. Overall, the material cycling and energy flow states of the Sanya and Changjiang coral reef ecosystems were stronger than those of Lingao, Wenchang, and Wanning, with lower fishing pressure in the former contributing to a more complex food web and enhanced community structural stability. This study provides the first systematic quantitative assessment of food-web structures across five distinct nearshore coral reef regions in Hainan, introducing an early-warning

Academic Editors: Tim Gray and Giuseppe Barbaro

Received: 29 May 2026
Revised: 9 July 2026
Accepted: 20 July 2026
Published: 24 July 2026

threshold for particulate inorganic carbon that offers direct, actionable reference for regional ecosystem-based management.

Keywords: coastal reefs; trophic transfer efficiency; keystone functional groups; ecosystem stability; environmental drivers

1. Introduction

Coral reef ecosystems are hailed as 'rainforests of the sea' due to their high biodiversity and multifaceted ecological contributions to fishery resources, coastal protection, and carbon cycling [1]. However, pressures such as global warming, ocean acidification, overfishing, and coastal development are leading to coral bleaching, degradation of community structure, and even phase shifts [2]. To address this large-scale ecological crisis, academia emphasizes that enhancing ecosystem resilience and protecting key functional groups like reef corals and herbivorous fish to prevent phase shifts from coral dominance to algal dominance is an effective path to cope with uncertainty and abrupt ecological transitions [1,3]. Meanwhile, coral reefs are simultaneously affected by multiple human activities (fishing, coastal engineering, aquaculture wastewater) and climatic drivers (warming, bleaching, hypoxia, acidification), leading to complex changes in their structure and function. There is an urgent need to quantify their trophic structure and energy flow to support ecosystem-based management decisions [3,4]. However, coral reef systems in different regions exhibit significant variations in species composition, trophic level distribution, and energy flow pathways, which also reflects significant differences in the response capabilities and recovery potential of different ecosystems when facing environmental disturbances [2].

To quantify these complex ecological processes, the Ecopath with Ecosim (EwE) model has become an important tool for studying marine food-web structure and energy flow [5]. Based on the principle of mass balance, the EwE model can not only describe the system average state and calculate ecological indicators such as total primary production/total respiration (TPP/TR), trophic transfer efficiency, system connectivity index, and omnivory index, but also conduct temporal and spatial scenario simulations through Ecosim/Ecospace and evaluate input uncertainty through iteration and Bayesian resampling, thereby providing comparable quantitative assessments for management plans [5–7]. The EwE model can also be cross-validated with independent stable isotope analysis data to improve credibility [8].

In the South China Sea region, several studies have already used this method to reveal the current status and vulnerability of nearshore ecosystems. For example, research on the Daya Bay ecosystem in the South China Sea indicates that its primary–secondary producers are key functional groups for the ecosystem, and the overall system is in an immature or degraded state, with weak resistance to external disturbances [9]. Spatial distribution analysis of different habitats (coral reefs, seagrass beds, open sea) in the Qilianyu area of the Xisha Islands shows that coral reefs have the highest diversity and stability, while seagrass beds played a prominent role in supporting biomass [10]. Another study in the Xisha Islands further explored the dual impacts of ocean warming and fishing pressure on system structure and catch, revealing that by mid-century, the combined effects of warming and fishing will lead to a significant decline in total catch and trophic levels [11].

Internationally, simulation studies targeting areas such as the Caribbean coast and the Eastern Pacific have also revealed that multiple stressors often synergistically lead to declines in both corals and small to medium-sized fish, while the biomass of certain large invertebrates may temporarily increase. However, overall biodiversity and fishery resources showed a downward trend [6]. Furthermore, under ocean warming scenarios, the total

biomass of pristine inshore coral reef ecosystems in the Western Atlantic decreases, and trophic transfer efficiency declines, foreshadowing a shift of the system towards a "carbon source" function and increased dependence on external subsidies, thereby weakening the ecosystem resilience [12]. However, a systematic food-web model study integrating multiple nearshore reefs to disentangle the relative effects of fishing pressure and environmental forcing is still lacking.

Existing assessments of the health status of coral reef ecosystems in Wenchang, Hainan, point to marine engineering construction and aquaculture wastewater discharge as the main drivers of coral degradation, but they have not deeply revealed the energy flow of food webs and the roles of functional groups [13]. The nearshore coral reefs in Hainan face diverse environmental drivers, including terrestrial nutrient input, changes in seawater temperature and salinity, and sediment particle characteristics. A systematic food-web model study is still lacking to understand how these factors regulate overall ecological stability by affecting functional group biomass and energy flux.

In summary, to fill the gap in the quantitative assessment of nearshore coral reef ecosystems in Hainan, this study intends to construct a mass-balance model of Hainan's nearshore coral reefs based on the EwE This will analyze the biomass distribution, energy flow pathways, and trophic structure of different functional groups. Simultaneously, combined with satellite environmental monitoring data, it will quantitatively assess the relationships between environmental variables with temperature, salinity, light, and organic matter characteristics on energy flow and system maturity. Specifically, we ask whether the among-reef differences in structure and function are governed primarily by fishing pressure or by environmental forcing, and which environmental variables are the dominant regulators. Accordingly, we test three hypotheses: (H1) differences in trophic structure and energy flow are driven primarily by fishing pressure, such that reefs under lower fishing pressure exhibit higher trophic levels, transfer efficiency, and maturity; (H2) key environmental variables—particularly Pic, Chl_a, and Sst—significantly regulate ecosystem structure and energy flow, with Pic being the dominant driver; and (H3) the effect of Pic on ecosystem function is non-linear, with an optimal range that maximizes energy flow and biomass. Our results demonstrate that the Sanya and Changjiang reefs exhibit greater maturity and stability, whereas the Lingao, Wenchang, and Wanning reefs are more vulnerable, with these differences driven primarily by fishing pressure and particulate inorganic carbon. By coupling trophic modeling with environmental drivers, this study aims to translate abstract energy-flow metrics into practical thresholds for ecosystem managers. The research results provide a scientific basis for the differentiated ecological conservation and sustainable fishery management of Hainan nearshore coral reefs.

2. Materials and Methods

2.1. Study Area and Basic Data Collection

The study area selected typical coral reef distribution areas around Hainan Island, including the nearshore sea of Sanya (SY), Changjiang (CJ), Lingao (LG), Wenchang (WC), and Wanning (WN) (Figure 1). Hainan Island is located in the northern part of the South China Sea and possesses abundant coral reef resources, making it an important coral reef distribution in China [13]. In recent years, due to human activity impacts such as climate change, marine pollution, overfishing, and coastal development, the Hainan nearshore coral reef ecosystem faces severe degradation pressure.

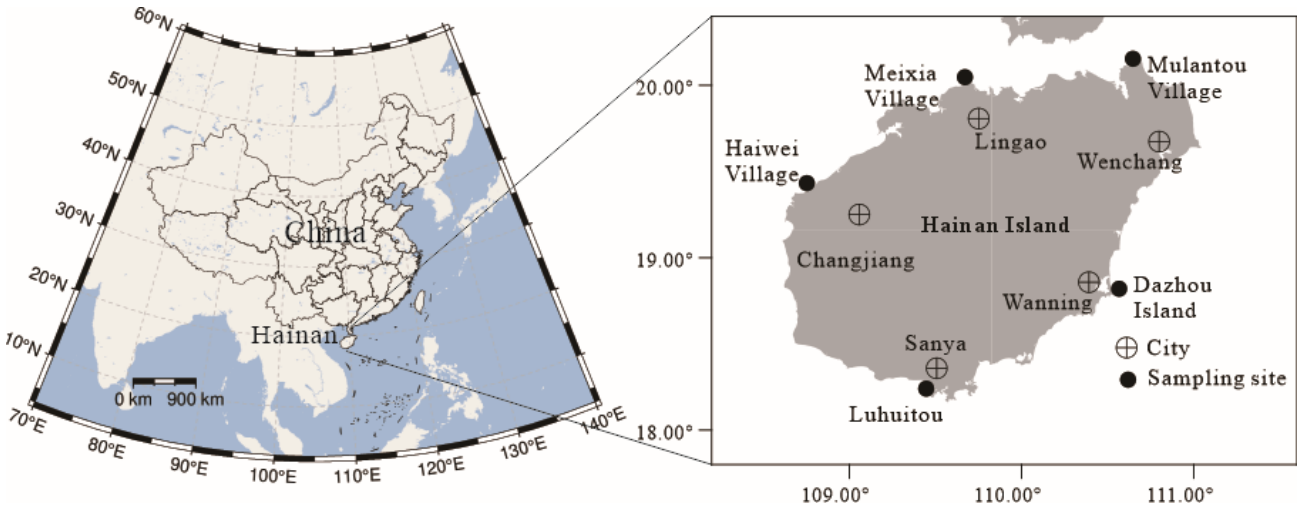

Figure 1. Sampling stations for the Hainan Island nearshore coral reef ecosystem.

The five regions were selected for three reasons. First, they are the principal areas of nearshore scleractinian-coral distribution around Hainan Island and are therefore representative of the island's coastal reef resources. Second, they are distributed across different coasts of the island (Sanya in the south, Changjiang and Lingao along the western/northwestern coast, Wenchang in the northeast, and Wanning in the southeast), so they experience contrasting oceanographic regimes, terrestrial runoff, and nutrient loading. Third, and most importantly for our hypotheses, they differ markedly in the type and intensity of human activity, allowing the relative contributions of fishing pressure and environmental forcing to be disentangled. Specifically, the regions form an anthropogenic-pressure gradient: Sanya is a major tourism and diving center with comparatively regulated fishing; Changjiang, on the less-urbanized western coast, is subject to relatively lower fishing pressure; Lingao is a center of intensive mariculture with elevated nutrient input and fishing intensity; Wenchang is strongly affected by marine engineering construction and aquaculture-wastewater discharge, previously identified as the main drivers of coral degradation there [13]; and Wanning, on the southeastern coast, is exposed to coastal tourism and artisanal fishing. They also form an environmental gradient, as reflected in the among-site differences in the satellite-derived variables quantified in this study (particulate inorganic carbon, chlorophyll-a, sea surface temperature, light diffuse attenuation coefficient, and salinity; see Supplementary Table S14). This gradient design is what enables the test of hypotheses H1 and H2. Table S14 summarizes the geographic setting, dominant anthropogenic pressures, key environmental characteristics, supporting references, and regional fishery statistics for each study region.

Sample collection was conducted from February to April 2023. Sampling in Sanya, Changjiang, Lingao, and Wenchang began in February. Due to weather conditions at the end of February, supplementary sampling in Wanning was carried out in April. Since February and April both fall within Hainan's northeast-monsoon (dry) season and the annual temperature of the island range is small, environmental conditions during this period were relatively stable, and the data collected across all regions were treated as a single synoptic survey suitable for mass-balance Ecopath modeling.

Three replicates were set in each region based on the characteristics of coral reef distribution. Coral reef biological samples were collected using a combination of the line transect method and quadrat survey method. At each region we conducted [line-intercept/belt] transects for benthic and coral cover, quadrats for benthic macro-organisms, gillnet deployments for the fish assemblage, and plankton net tows for phytoplank-

ton (Supplementary Table S15). Zooplankton data were collected using vertical trawling according to the GB/T 12763.9 (2007) [14] to calculate biomass per unit volume (Supplementary Figure S1 and Table S1). In addition, some data not obtained for the subsequent model construction came from similar coral reef Ecopath models. Phytoplankton biomass (g/m^2) was calculated based on Brown et al. and Shang et al., using SCS chlorophyll concentrations (mg/m^3) [15–17]. Due to the lack of biomass data for cartilaginous fish and benthic producers (turf and macroalgae), output parameters from similar models were used [18]. To balance our model, EE values for each biomass were set to 0.189, 0.239, and 0.375, respectively, and these values were input into model to calculate the biomass of missing functional groups [8,18–20]. The values 0.189 and 0.239 were adopted from the Xisha coral reef Ecopath model [21], and 0.375 was adopted from the Yongxing coral reef Ecopath model [22]. EE values were not chosen arbitrarily: they were adopted from published Ecopath models of tropical coral reef ecosystems at comparable latitudes and with similar ecosystem characteristics, in which cartilaginous fish and benthic producers (turf and macroalgae) occupy analogous trophic roles [8,18–20]. Biomass data for other functional groups (e.g., detritus) were derived from particulate organic carbon from satellite data (https://oceandata.sci.gsfc.nasa.gov/l3/order/, accessed on 28 May 2026), with values close to the amount of detritus in adjacent waters [23]. To allow comparison across regions of different reef extents, sampling effort was standardized by expressing all quantitative data on a per-unit-area (or per-unit-effort) basis before they were used as inputs for the Ecopath models.

Methods for estimating P/B include population resource assessment, the natural mortality (M) method, and the fishing mortality method. According to bioenergetic theory, the production (P)/consumption (Q) ratio (P/Q) is assumed to be 0.1–0.3. Under the assumption of a mass-balanced trophic model, the P/B of "fish" is equal to the instantaneous total mortality (Z) [24]. The Q/B for each fish functional group was estimated according to Palomares and Pauly [25]; P/B and Q/B for certain functional groups were estimated based on Fishbase (https://www.fishbase.org) and parameters from tropical coral reef models in similar latitudes or with similar ecosystem characteristics [9,19,20,26–28].

We recorded the latitude and longitude of each sampling station and accessed corresponding satellite environmental monitoring data for the time points from the EU's Global Ocean Physical Analysis and Forecast ocean satellite (https://data.marine.copernicus.eu/product/GLOBAL_ANALYSISFORECAST_PHY_001_024/download, accessed on 28 May 2026) and the OceanColor data website (https://oceandata.sci.gsfc.nasa.gov/l3/order/, accessed on 28 May 2026). The source files and R code of extracting environmental data for each sampling point were freely available at https://github.com/xupeng520qxm/HNDenv/tree/main, accessed on 28 May 2026.

2.2. Model Construction

We used EwE 6.7 software to construct five Ecopath models representing the nearshore coral reef ecosystems in different regions around Hainan Island during the same quarter [29]. In an Ecopath model, functional groups with similar trophic levels, life histories, and niche characteristics must be comprehensively considered, and all functional groups must include the basic processes of energy and material flow in the ecosystem [5]. The Ecopath model includes two main equations—the first, Equation (1), defines the balance between input and output for each functional group to ensure that the ecotrophic efficiency does not exceed 1. Equation (2) defines the thermodynamics of the functional groups. The expressions for Equation (1) and Equation (2) are:

$$B_i \times \left(\frac{P}{B}\right)_i \times EE_i = Y_i + \sum_{j=1}^{n} B_i \times \left(\frac{Q}{B}\right)_i \times DC_{ji} + B_i \times BA_i \quad (1)$$

$$Q_i = P_i + R_i + U_i \quad (2)$$

where B_i is the biomass of group i; $(P/B)_i$ is the production-per-unit biomass of group i, which is equal to the total mortality rate of group i; EE_i is the ecotrophic efficiency of group i, defined as the fraction of production consumed within the system or taken by fisheries; Y_i is the total catch rate of group i; $(Q/B)_j$ is the consumption-rate-per-unit biomass of group j; DC_{ij} is the fraction of prey i in the average diet of predator j; BA_i is the biomass accumulation rate of group i; E_i is the net migration rate (inflow and outflow); Q_i is the consumption of group i; R_i is the respiration of group i; and U_i is the unassimilated food of group i.

The identification of Ecopath functional groups needs to consider changes in life history stages, habitat, and/or diet. Therefore, functional groups can be represented as a single biomass pool or multi-stanza functional groups [30]. In this study, the components in the Ecopath models for different regions of the nearshore coral reef ecosystem around Hainan Island can be divided into 16 groups for Sanya, 14 for Changjiang, 16 for Lingao, 17 for Wenchang, and 15 for Wanning. Among these, 7 groups are fish groups, 4 are invertebrate groups, and the remaining 6 groups include sea turtles, zooplankton, phytoplankton, macroalgae, turf algae, and detritus, covering the energy flow processes at various trophic levels of each ecosystem. The selection of these functional groups was based not only on field survey results but also on ecology, biosystematics, feeding habits of species, and species distribution [31]. Fish species were assigned to functional groups based on similar ecological characteristics (e.g., diet, predator, body size, and metabolic requirements). The group names for carnivorous fish functional groups were based on size classification (small for <10 cm, medium for 10–20 cm, and large for >20 cm). The carnivorous fish were divided into small (<10 cm), medium (10–20 cm), and large (>20 cm) size classes because body size is a primary determinant of trophic role in reef fishes, and these classes correspond to ecologically distinct feeding niches. These thresholds are also consistent with size-class conventions widely used in Western Pacific/Indo-Pacific coral-reef fish studies, in which breakpoints at approximately 10 cm and 20 cm are commonly applied in visual-census and trophic analyses to separate small, intermediate, and large individuals [26,27]. In addition, the thresholds were checked against the length-frequency distribution of our own sampled catch and against length-at-maturity information from FishBase for the dominant carnivorous species, confirming that the 10 cm and 20 cm breakpoints fall close to natural discontinuities in the size structure and approximate the transition from juvenile to mature stages.

2.3. Fishery Catch, Dietary Composition and Model Debugging

The Hainan Provincial Fishery Statistical Yearbook does not record fishery data for the Xisha Islands, and the fishing pressure on the Xisha Islands mainly comes from different prefectural-level cities on Hainan Island. We selected the average fishery catch data from the five aforementioned regions in the 'Hainan Statistical Yearbook 2019' as the baseline for the Xisha Islands' fishery data [32]. This was then combined with the 2019 fishery catch data from the Qilianyu coral reefs in the Xisha Islands [21], along with fishery data from the 'Hainan Provincial Statistical Yearbook 2019' and 'Hainan Provincial Statistical Yearbook 2023', to estimate the catch of coral reef fish and some invertebrates in the nearshore coral reefs of Hainan Island [32,33] (Tables S8–S12).

Since diet matrices are important for Ecopath simulations, the diets of different functional groups were reconstructed based on stomach content analysis, published literature, and Fishbase (www.fishbase.org) (Tables S3–S7) [22]. Given that the nearshore coral reefs of Hainan Island are an open ecosystem, the 'diet import' method needs to be adopted for certain functional groups [29]. Additionally, biological differences often lead to unassimi-

lated consumption by herbivorous fish, benthic invertebrates, and zooplankton compared to other animals [27]; the Un. Q for crustaceans, zooplankton, and herbivorous fish was set at 0.25, 0.30, and 0.40, respectively [21].

Before balancing or running, the pre-balance diagnostic was used to check consistency of the model. Output parameters that needed adjustment included: EE (<1.0), total gross efficiency (P/Q, 0.1–0.3), net efficiency (NE, NE − P/Q > 0), respiration/assimilation biomass (R/AS, <1.0), respiration/biomass (R/B, fish: 1-10; high turnover populations: 50–100), and production/respiration (P/R, <1.0 or >1.0) [34,35]. The model is adjusted to reach equilibrium according to thermodynamic principles. In addition, sensitivity analysis is performed to test how small changes in input data affect model output parameters [36].

2.4. Data Analysis

2.4.1. Mixed Trophic Impact (MTI) and Keystone Index Analysis

The Ecopath MTI model quantified the direct and indirect trophic effects among functional groups, assessing the positive or negative impact of biomass changes in one functional group on all other components of the coral reef ecosystem and analyzing the interactions between functional groups and fishing activities [37]. Keystone index analysis, based on MTI, identifies functional groups within the food web that have high overall impact and relatively low biomass [38].

2.4.2. Model Characteristic Analysis

Based on the Ecopath model equilibrium results, ecosystem-wide characteristic parameters reflecting the scale, stability, and maturity of the nearshore coral reef ecosystem of Hainan Island, calculated using network analysis, such as the total system throughput, including the sum of all consumption, all exports, all respiration flows, and all detritus flows, can be used to quantify the ecological scale and 'metabolic level' of the ecosystem [39,40]. System descriptive indices, such as the ratios of total primary production/total respiration (TPP/TR) and total primary production/total biomass (TPP/TB), Finn's cycling index (FCI), and Finn's Mean Path Length (MPL), characterize ecosystem maturity [29,39,41]. The closer TPP/TR is to 1, the more stable the ecosystem.

The cycling of matter is also a key process for the functioning of natural ecosystems, as it promotes homeostatic control over flow magnitudes [41]. FCI and MPL increase with ecosystem maturity [42]. Food-web complexity and omnivory index are often used to assess ecosystem stability; the Connectance index (CI) is the ratio of actual links to possible links in a given food web, and the system omnivory index (SOI) is an average omnivory index of all consumers, weighted by the logarithm of each consumer food intake [29]. Both the CI and SOI indicate the complexity of internal connections within the ecosystem; when their values approach 1, the internal relationships of the food web composed of functional groups are more likely to be complex, and the ecosystem is more stable [29]. Ascendency (A) integrates both size and organization (the number and diversity of interactions between ecosystem components) [29]; the relative overhead (O/C) is used as an index of ecosystem resilience [43].

2.4.3. Environmental Factor-Associated Analysis

This study used various statistical methods (correlation, Principal Component Analysis, and multiple regression) to analyze the relationships among different ecosystem structures, functions, and environmental factors. First, by calculating the correlation matrix between environmental factors and ecological indicators, a multiple regression analysis was performed for each ecological indicator against environmental factors, and standardized coefficients were extracted. Principal Component Analysis (PCA) was used to reduce the dimensionality of environmental variables and identify main environmen-

tal factors affecting coral reef ecosystems. Second, we standardized coefficients of each associated indicator and calculated a comprehensive mean score to identify consistently important environmental factors across different analytical methods. Finally, a Generalized Additive Model was used to detect whether there are non-linear relationships among variables. All statistical analyses were performed using R 4.2.1 software, with the significance level set at $p < 0.05$. R language code and data are freely available at https://github.com/xupeng520qxm/HNDenv/tree/main, accessed on 28 May 2026.

3. Result

3.1. Trophic Structure and Biomass Recycle

According to PREBAL diagnostic and sensitivity analysis of the Ecopath models for nearshore coral reef ecosystems in Hainan Island, the model fit is good (Supplement File S1: Text S1, Figure S6). The input and output parameters for the functional groups of the nearshore coral reef Ecopath models at five sites in Hainan Island are shown in Supplement File S2: Tables S8–S12. The trophic level (TL) values for all functional groups conform to basic ecological principles, ranging from 1.00 to 5.00 (Figure 2), with more than half of functional group TLs concentrated between the second and fourth TL. Coral reef systems at each location exhibited relatively distinct material flows and TL differences, reflecting diversity and complexity of ecological functions among regions. Specifically, Figure 2 shows that internal energy flows within each system present differentiated paths and intensities, indicating significant differences in the dependence on material cycling and ecological connectivity among coral reef ecosystems at different locations. Figure 2a,b show that in Sanya and Changjiang, corals were main energy source for mollusks, while Figure 2c–e show that in Lingao, Wenchang, and Wanning, phytoplankton were the main energy source for zooplankton. Mollusks were also the main energy source for fishing in all five ecosystems, with Lingao, Wenchang, and Wanning having relatively higher energy flows from mollusks to fishing, suggested potentially higher mollusk fishing intensity. In Figure 3a, a comparison of the sum of all flows into detritus (SAFID) and total system throughput (TST) at different locations reveals that Lingao (SAFID: 3918.97 $t \cdot km^{-2} \cdot a^{-1}$, TST: 11,325.72 $t \cdot km^{-2} \cdot a^{-1}$) and Wenchang (SAFID: 9746.32 $t \cdot km^{-2} \cdot a^{-1}$, TST: 29,724.00 $t \cdot km^{-2} \cdot a^{-1}$) have a higher total detritus inflow and system throughput, reflected stronger material and energy exchange activity. Figure 3b displays the average trophic level of catches (mTlc) at each location, showing that the mTlc in Sanya and Changjiang was greater than 3.0, while it was less than 3.0 at the other three locations. This implies that the food chain structure in the former was more complex and includes higher trophic-level groups, which indirectly explains that the relatively higher mollusk fishing energy in Lingao, Wenchang, and Wanning might be due to the lower biomass of high trophic-level groups. In Figure 3c, the system omnivory index (SOI) and Shannon diversity index (SDI) respectively reflect the dietary diversity of species and community diversity within the ecosystem. The results indicate that the Sanya and Changjiang coral reef systems had relatively higher SOIs, 0.62 and 0.80, respectively, exhibiting a more complex food-web structure. However, the Lingao, Wanning, and Changjiang coral reef systems had higher SDIs, 2.14, 1.98, and 1.98, respectively, indicating higher biodiversity. Furthermore, Figure 3d compares the FCIs and MPLs of coral reef ecosystems at different locations. The data show that Sanya has larger FCIs and MPLs, 7.69 and 2.53, indicating that its ecosystem energy flow has a higher recycling efficiency and a longer stable path, suggesting higher system maturity and stability.

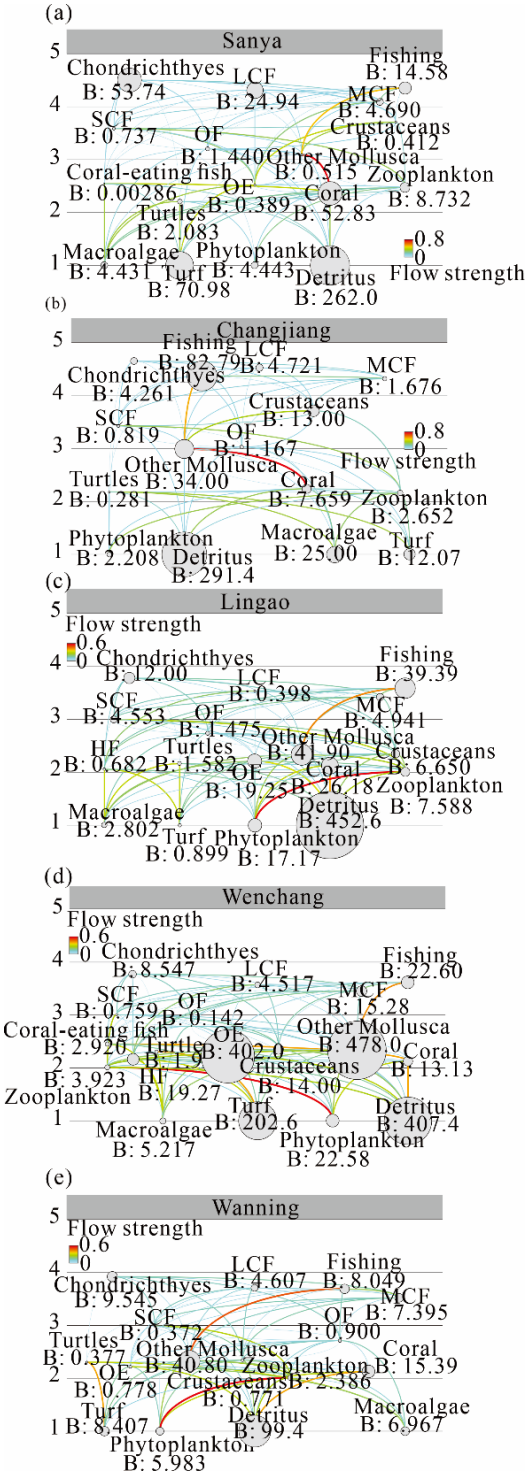

Figure 2. Trophic flow diagrams of the Ecopath models for the five nearshore coral reef regions in Hainan: (**a**) Sanya, (**b**) Changjiang, (**c**) Lingao, (**d**) Wenchang, and (**e**) Wanning. In each diagram, circles represent functional groups, positioned along the vertical axis according to their trophic level; the area of each circle is proportional to the group's biomass, and the biomass value (B, t·km^{-2}) is given next to each node. Lines represent the energy flows among functional groups, with line color indicating the relative flow strength according to the color bar shown in each panel (note that the range of the color scale differs among panels). "Fishing" denotes the fishery (catch) compartment. The number of functional groups varies among regions (14–17), reflecting differences in species composition recorded during the field surveys. LCF: large carnivorous fish. MCF: medium carnivorous fish. SCF: small carnivorous fish. OE: other echinoderms. OF: omnivorous fish. HF: herbivorous fish.

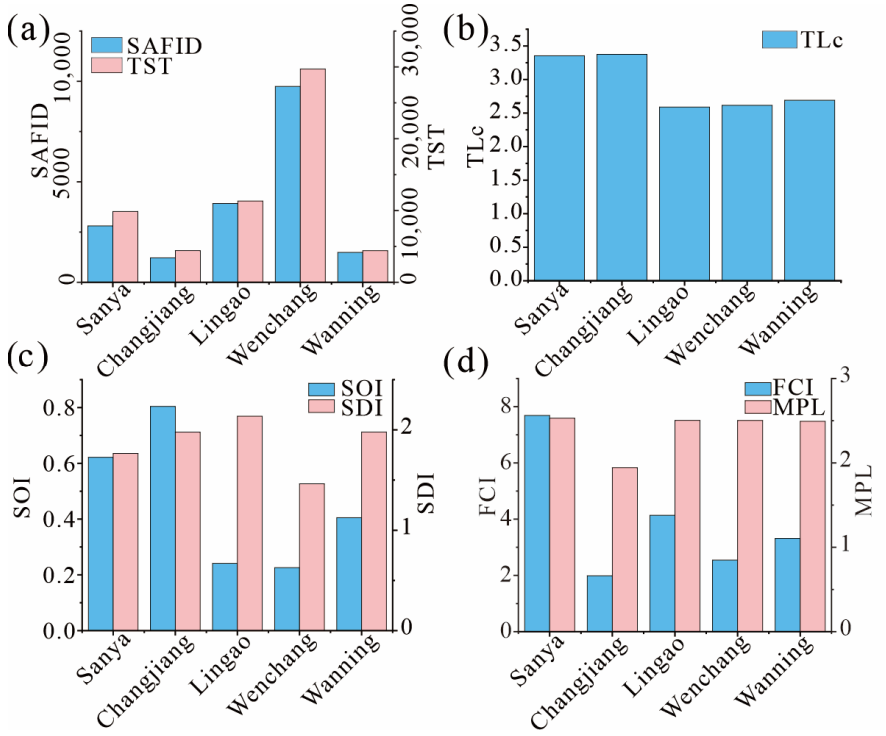

Figure 3. Ecosystem-level network indices of the Ecopath models for the five nearshore coral reef regions in Hainan (Sanya, Changjiang, Lingao, Wenchang, and Wanning). (**a**) Sum of all flows into detritus (SAFID, t·km^{-2}·a^{-1}; left axis) and total system throughput (TST, t·km^{-2}·a^{-1}; right axis); (**b**) mean trophic level of the catch (TLC); (**c**) system omnivory index (SOI; left axis) and Shannon diversity index of flows (SDI; right axis); (**d**) Finn's cycling index (FCI, %; left axis) and mean path length (MPL; right axis). In panels (**a**,**c**,**d**), blue bars correspond to the lefthand axis and pink bars to the righthand axis. In panels (**c**,**d**), parameters are paired on dual axes to facilitate the direct comparison of ecologically interrelated metrics: SOI (trophic-web complexity) and SDI (community diversity) jointly characterize ecosystem structural heterogeneity, while FCI (cycling efficiency) and MPL (energy flow path length) are complementary Finn indices that collectively indicate ecosystem maturity.

3.2. Energy Flow

Food-web analysis confirmed that Sanya and Changjiang have Lindeman trophic flow pathways with five integrated TLs, while Lingao, Wenchang, and Wanning have Lindeman trophic flow pathways with four integrated TLs (Table 1). The "total flow" at each TL significantly decreased as the TL increased. The throughput generated by TL I and II at different locations accounted for 90.04% in SY, 78.15% in CJ, 91.91% in LG, 93.94% in WC, and 92.91% in WN, which is consistent with the principle of the energy pyramid. As the main energy source, the proportion of consumption by TL I predators to the total predator consumption at each location was 69.23%, 64.00%, 89.03%, 77.44%, and 83.19%, respectively. The proportion of TL I flow to detritus to the total flow to detritus was 67.52%, 67.24%, 75.88%, 81.70%, and 79.29%, respectively. This indicated that TL I energy utilization efficiency was low, and most of the energy was stored as detritus at lower TLs, failing to effectively transfer upwards. However, we could observe that the proportions of consumption by TL I predators and flow to detritus in Sanya and Changjiang were lower compared to the other three points. This suggested that a larger proportion of energy flowed to higher trophic levels and less energy flowed to detritus, which is consistent with the aforementioned research results regarding higher trophic levels of catches and higher food-web complexity and stability.

Table 1. Distribution of flow in the coastal coral reef ecosystem of Hainan Island. SY: Sanya, CJ: Changjiang, LG: Lingao, WC: Wenchang, WN: Wanning. All flow values are expressed in $t \cdot km^{-2} \cdot a^{-1}$.

Trophic Level	Area	Consumption by Predators	Export	Flow to Detritus	Respiration	Throughput
V	SY	11.59	0.17	41.89	14.89	68.55
	CJ	4.68	4.54	11.63	28.55	49.40
	LG	-	-	-	-	-
	WC	-	-	-	-	-
	WN	-	-	-	-	-
IV	SY	36.38	0.40	98.33	45.64	180.80
	CJ	26.40	14.65	40.80	91.39	173.20
	LG	4.76	2.31	8.95	25.63	41.65
	WC	7.76	1.39	22.04	53.67	84.87
	WN	6.12	0.65	10.05	30.10	46.92
III	SY	112.50	0.59	198.30	143.80	455.30
	CJ	95.23	24.52	64.21	127.70	311.60
	LG	29.88	10.56	49.63	114.90	205.00
	WC	85.29	6.04	299.40	565.80	956.60
	WN	26.58	2.24	27.25	64.50	120.60
II	SY	353.70	0.74	548.60	484.20	1387.00
	CJ	177.00	8.80	246.60	226.50	659.00
	LG	179.80	16.94	807.30	736.80	1741.00
	WC	1169.00	9.50	1342.00	1999.00	4519.00
	WN	92.43	3.06	246.70	255.20	597.30
I	SY	1170.00	2242.00	1896.00	0.00	5309.00
	CJ	541.30	0.00	749.00	0.00	1290.00
	LG	1744.00	0.00	2730.00	0.00	4474.00
	WC	4332.00	0.00	7440.00	0.00	11,772.00
	WN	622.70	0.00	1095.00	0.00	1718.00
Sum	SY	1690.00	2244.00	2808.00	695.50	7437.00
	CJ	845.80	53.90	1114.00	479.80	2494.00
	LG	1959.00	30.04	3598.00	881.90	6468.00
	WC	5594.00	17.10	9106.00	2625.00	17,342.00
	WN	748.50	6.03	1381.00	356.40	2492.00

The energy transfer efficiency of TL refers to the ratio of its energy output and intake to its throughput, representing the energy efficiency of the TL in the ecosystem. Table 2 shows that the geometric mean of the energy transfer efficiency for TL II–IV at each location was 24.49%, 30.25%, 15.98%, 24.57%, and 18.04%, respectively, which is significantly higher than Lindeman's trophic transfer efficiency (10%) (Figure 4). It was also found that the transfer efficiencies in Sanya, Changjiang, and Wenchang were higher than in Lingao and Wanning, indicating stronger internal energy flow, which has a certain promotional effect on improving their internal ecosystem conditions. Additionally, we found that the transfer efficiencies from primary producers in Sanya, Changjiang, and Wenchang were 24.34%, 29.69%, and 24.42%, respectively, which were lower than their transfer efficiencies from detritus, indicating that their ecosystems are dominated by detrital food chains. In contrast, the transfer efficiencies from primary producers in Lingao and Wanning were 16.00% and 18.11%, respectively, which were higher than their transfer efficiencies from detritus, indicating that their ecosystems are dominated by grazing food chains. It was speculated that, for the coral reef ecosystems of Hainan Island, detrital food-chain-dominated ecosystems play a positive role in improving the overall utilization efficiency of the ecosystem.

Table 2. Trophic transfer efficiency of the coastal coral reef ecosystem of Hainan Island. SY: Sanya, CJ: Changjiang, LG: Lingao, WC: Wenchang, WN: Wanning.

Source	Area	Trophic Level			
		II	III	IV	V
Producer	SY	25.66	25.88	21.71	18.88
	CJ	30.44	38.88	22.12	16.73
	LG	11.30	19.73	16.97	-
	WC	25.66	25.88	21.71	-
	WN	15.99	23.90	14.44	-
Detritus	SY	25.85	27.64	22.06	17.94
	CJ	49.66	49.42	13.52	22.40
	LG	10.85	19.82	17.09	-
	WC	25.85	27.64	22.06	-
	WN	17.04	22.35	14.24	-
All flows	SY	25.7	26.23	21.79	18.67
	CJ	34.23	42.1	19.21	18.02
	LG	11.17	19.75	17.01	-
	WC	25.70	26.23	21.79	-
	WN	16.29	23.44	14.38	-

Notes: Total flow proportion from detritus: SY: 0.45, CJ: 0.42, LG: 0.42, WC: 0.39, WN: 0.42; transfer efficiency (mTE, calculated as the geometric mean of TL II–IV); from primary producers: SY: 24.34%, CJ: 29.69%, LG: 16.00%, WC: 24.42%, WN: 18.11%; from detritus: SY: 25.07%, CJ: 32.14%, LG: 15.92%, WC: 25.18%, WN: 17.88%; total: SY: 24.49%, CJ: 30.25%, LG: 15.98%, WC: 24.57%, WN: 18.04%.

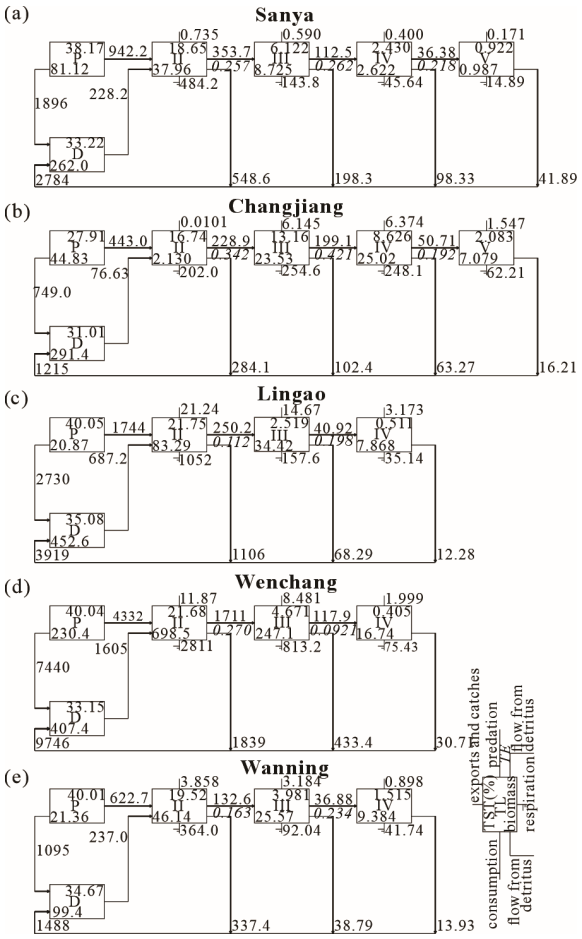

Figure 4. Lindeman trophic flow pathways of the Hainan Island coastal coral reef ecosystem based on ecological pathways. P: primary producers; D: detritus; II–V: trophic levels; TST: total system throughput; TE: transfer efficiency; TL: trophic level.

3.3. MTI and Keystone Index

Figure 5, through a combined analysis of the MTI and the keystone index, reveals the directional impact and criticality of different functional groups on the trophic web within the nearshore coral reef ecosystems of Hainan Island. MTI analysis (Figure 5a–e) showed that primary producers (phytoplankton, turf, and macroalgae) had a positive effect on most predators. Regarding corals, while benthic algae (turf and macroalgae) in Sanya and Changjiang had a certain promoting effect on corals, benthic algae in Lingao, Wenchang, and Wanning showed a significant inhibitory effect on corals. The food-web structures in Sanya and Wenchang indicated that corals have a significant promoting effect on coral-eating fish. Overall, fishing had a negative impact on most groups, with the negative impact of fishing in Sanya being weaker compared to that of the other regions. Fishing had a strong negative impact on medium and large fish in Changjiang, Lingao, Wenchang, and Wanning. Fishing intensity directly affects the structural condition of the coral reef ecosystem.

According to the keystone index (KS) and relative total impact (RTI), the critical functional groups in the coral reef ecosystems of different regions of Hainan Island were identified, with top-ranked functional groups considered key species in the system. Figure 5f–j reveal that zooplankton (KS = −0.040, RTI = 1.000) and corals (KS = −0.263, RTI = 0.748) in Sanya, zooplankton (KS = −0.059, RTI = 1.000) and corals (KS = −0.202, RTI = 0.793) in Changjiang, zooplankton (KS = −0.141, RTI = 1.000) and cartilaginous fish (KS = −0.216, RTI = 0.868) in Lingao, medium carnivorous fish (KS = −0.086, RTI = 1.000) and other echinoderms (KS = −0.2303, RTI = 0.903) in Wenchang, and medium carnivorous fish (KS = −0.156, RTI = 0.974) and other mollusks (KS = −0.327, RTI = 1.000) in Wanning were the critical functional groups in their respective regions. The high KS and RTI values of these functional groups indicated their important roles in their respective coral reef ecosystems, had a decisive impact on the trophic network structure and system integrity, and thereby provided a theoretical basis for maintaining and managing the trophic dynamics of coral reef ecosystems.

3.4. Key Correlating Factors

Figure 6 and Figures S2–S4 systematically reveal the influence of key environmental factors and their mechanisms on ecosystem structure (TST, TB), energy flow (mTE), ecosystem health (SDI, Sum of Production: SP, TPP/TR, FCI, MPL, Connectance index: CI, SOI), and fishery-management-related indicators (total catch: TC, mTlc) in Hainan Island. Firstly, Figure 6a compares the results of different methods for assessing the importance of environmental factors, indicating that particulate inorganic carbon (Pic), chlorophyll-a concentration (Chl_a), and sea surface temperature (Sst) were prominent influences across all indicators, validating their dominant role in system function. Figure 6b further integrates the extent of influence of various environmental factors on ecological indicators through a comprehensive score, highlighting the critical regulatory roles of particulate inorganic carbon, light diffuse attenuation coefficient, and chlorophyll-a concentration, with particulate inorganic carbon being the most important influencing factor. Correlation analysis based on the Generalized Additive Model revealed significant non-linear relationships between particulate inorganic carbon and total catch, total system throughput, total biomass, and total production (Figure 6c–f), with no significant non-linear relationships observed for other ecosystem parameters (Figure S5). Specifically, Pic showed a significant positive correlation with total carbon, with the rate of increase accelerating further when Pic concentrations exceeded 0.0125 mol/m^2. Conversely, Pic exhibited a peaked-curve relationship with total standing stock, total biomass, and species richness, indicating an optimal Pic range of 0.0050–0.0075 mol/m^2 for maximizing energy flow and biomass ac-

cumulation. These results support particulate inorganic carbon as an important driving force for ecosystem function and fishery productivity, with its influence realized through regulating energy flow and biological production processes.

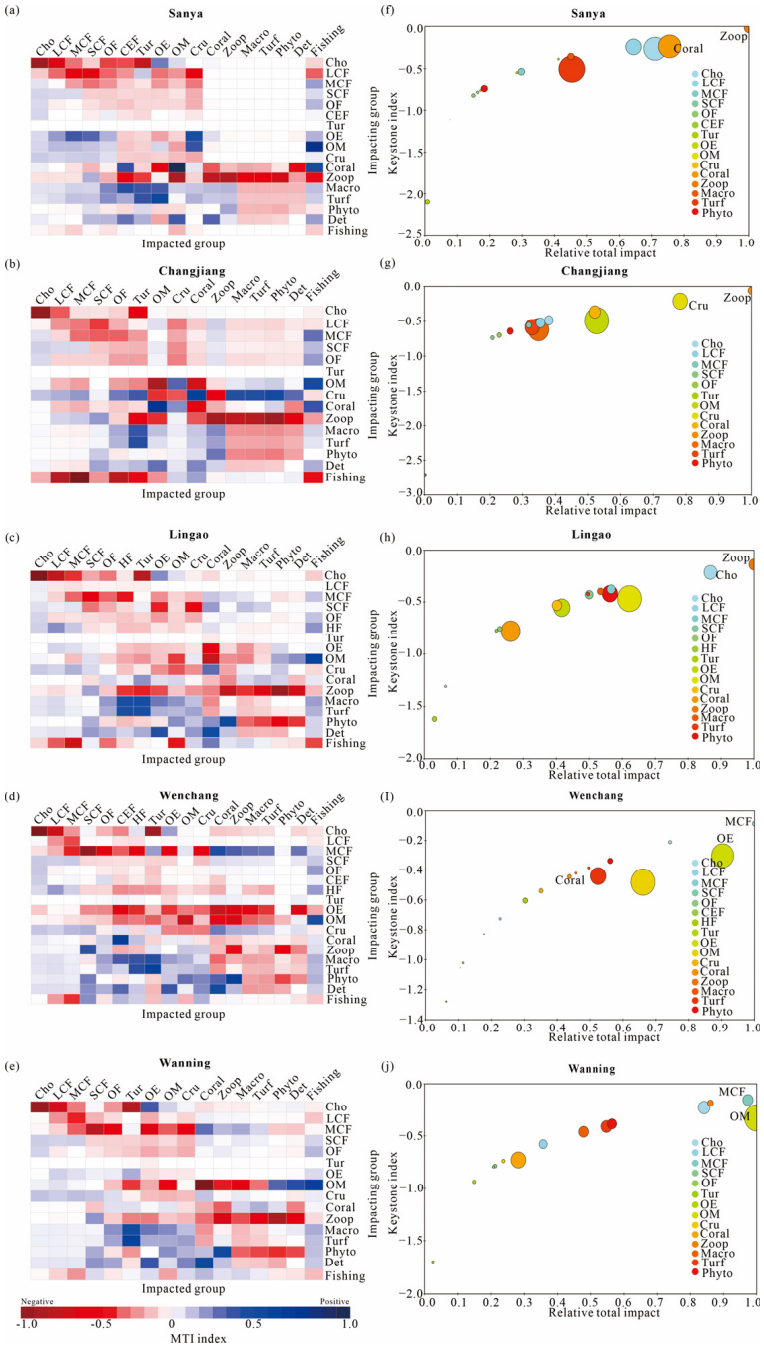

Figure 5. Mixed trophic impact (MTI) and keystone index (KS) of nearshore coral reefs on Hainan Island. (**a**–**e**) Positive (blue) and negative (red) values of the MTI index represent positive and negative impacts, respectively. (**f**–**j**) For each functional group, the keystone index (y-axis) corresponds to its relative total impact on the trophic web (x-axis). The total impact is relative to the maximum impact measured; the x-axis scale is between 0.0 and 1.0. Functional groups are sorted in decreasing order of the keystone index; thus, the key functional group is the top-ranked functional group. Circles are proportional to the biomass of the functional group in the system. Cho: Chondrichthyes; LCF: large carnivorous fish; MCF: medium carnivorous fish; SCF: small carnivorous fish; OF: omnivorous fish; CEF: coral-eating fish; HF: herbivorous fish; Tur: turtles; OE: other echinoderms; OM: other mollusks; Cru: crustaceans; Zoop: zooplankton; Macro: macroalgae; Phyto: phytoplankton.

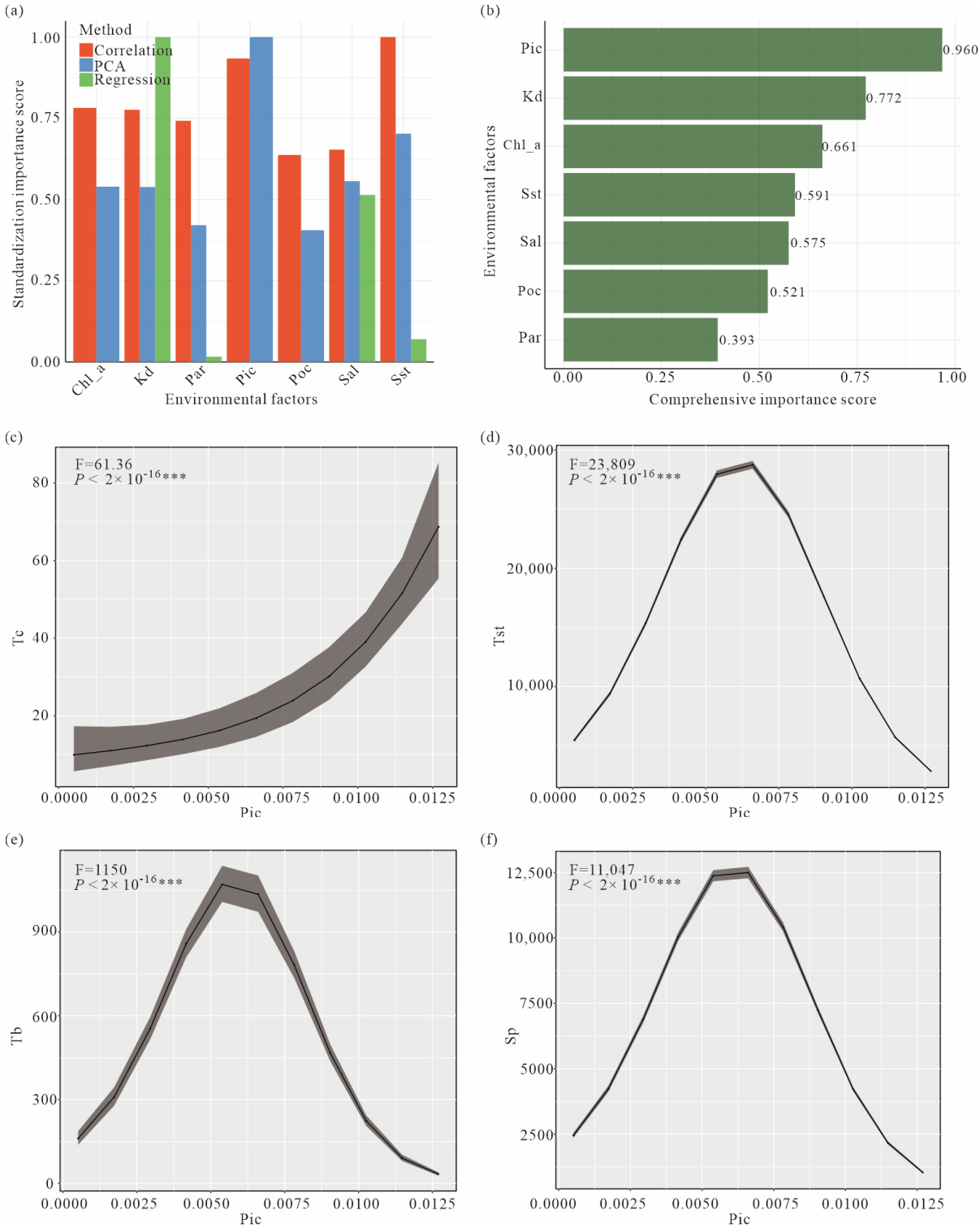

Figure 6. Key factors affecting the ecosystem structure, energy flow, ecosystem health, and fishery management indicators of Hainan Island. (**a**) Comparison of environmental factor importance assessed by different methods. (**b**) Comprehensive scores of environmental factor impacts on ecological indicators. (**c**–**f**) GAM-based correlation fitting curves of particulate inorganic carbon with Tc, Tst, Tb, and Sp. Chl_a: chlorophyll-a concentration, Kd: light diffuse attenuation coefficient, Par: photosynthetically active radiation, Pic: particulate inorganic carbon, Poc: particulate organic carbon, Sal: salinity, Sst: sea surface temperature, Tc: total catch, Tst: total system throughput, Tb: total biomass, Sp: total production. *** indicates $p < 0.001$.

4. Discussion

The objective of this study was to quantify the trophic structure, energy flow, and environmental drivers of Hainan's coastal coral reefs. The main finding is that the Sanya and Changjiang reefs exhibit greater maturity and stability, while those in Lingao, Wenchang, and Wanning are more vulnerable, with differences driven primarily by fishing pressure and particulate inorganic carbon.

4.1. Stability Analysis of Ecosystem Trophic Structure and Energy Flow

The Ecopath model of Hainan nearshore coral reefs constructed in this study showed that the trophic levels in different regions of the system range from primary producers (Trophic Level I) to top predators (Trophic Level 4.656), with the highest trophic levels in Sanya and Changjiang being 4.505 and 4.656, slightly higher than the 3.977 in Daya Bay and 3.80 in Qilianyu [9,21]. The highest trophic levels in Lingao, Wenchang, and Changjiang were 3.780, 3.776, and 3.924, which were close to those in Daya Bay and Qilianyu [9,21]. In our study, the mean trophic level of catch for Sanya and Changjiang was 3.355 and 3.376, slightly higher than the 2.727 in Daya Bay and 2.62 in Qilianyu, while the MTL for Lingao, Wenchang, and Changjiang was 2.59, 2.616, and 2.691, which were close to those in Daya Bay and Qilianyu [9,21]. The combination of these two factors reflects the differences in fishing selectivity and ecosystem maturity in Sanya and Changjiang, and was also closely related to conservation management and fishing intensity [9,44]. A higher trophic level of catch generally indicates that fish resources are relatively underexploited, but if the biomass of high trophic level organisms is low, it could easily lead to unstable ecosystem structure and ecological function degradation [45].

The average trophic transfer efficiencies calculated by our model were 24.49%, 30.25%, 15.54%, 13.96%, and 17.64% in SY, CJ, LG, WC, WN, which were significantly higher than the 10.9% in Daya Bay and 13.15% in the Qilianyu coral reefs [9,21]. However, the total primary production/total respiration (TPP/TR) and total primary production/total biomass (TPP/TB) ratios for each location (TPP/TR: SY for 1.99, CJ for 1.95, LG for 3.23, WC for 2.80, WN for 3.39; TPP/TB: SY for 12.50, CJ for 11.52, WC for 8.68, WN for 16.41) were significantly lower than those of Daya Bay (TPP/TR = 3.5, TPP/TB = 82.5) and Qilianyu (TPP/TR = 3.79, TPP/TB = 26.3), with the exception of Lingao's TPP/TR of 27.28, which was slightly higher than that of Qilianyu [9,21]. This indicated a certain efficiency loss in the production–respiration balance and biomass utilization of Hainan nearshore coral reefs.

The variations in primary producer communities across different ecosystems and their mechanisms of impact on secondary consumers may be influenced by local environmental conditions and the extent of anthropogenic disturbance. The relevant literature indicates that foundation species, such as corals and large phytoplankton, play a decisive role in the energy flow and stability of ecosystems [3]. Specifically, coral-based food chains in Sanya and Changjiang may have enhanced detrital energy flow, whereas phytoplankton-driven grazing food chains in the coral reef ecosystems of Lingao, Wenchang, and Wanning might affect the efficiency of energy cycling. Lingao (SAFID: 3918.97 $t \cdot km^{-2} \cdot a^{-1}$, TST: 11,325.72 $t \cdot km^{-2} \cdot a^{-1}$) and Wenchang (SAFID: 9746.32 $t \cdot km^{-2} \cdot a^{-1}$, TST: 29,724.00 $t \cdot km^{-2} \cdot a^{-1}$) exhibited high detrital inflow and total system throughput, respectively. This suggested active material and energy cycling within their ecosystems and a high responsiveness to external inputs and disturbances. However, this elevated throughput might be associated with intensified detrital pathways under specific fishing or environmental pressures [21,46], which could also account for the lower complexity and stability of their food webs compared to those of Sanya and Changjiang. Sanya and Changjiang demonstrate stronger omnivory and more complex food-web structures, with SOI values of 0.62 and 0.80, respectively. This indicated that while complex

trophic cross-links have formed in certain areas, there was considerable variation in species richness, reflecting the functional and structural heterogeneity of these ecosystems. Mature and stable coral reef ecosystems typically possess higher rates of energy cycling and longer food chain pathways, thereby exhibiting greater resilience to environmental perturbations. Omnivorous behavior contributes to enhanced food web stability, energy redistribution, maintenance of ecosystem services, and improved recovery capacity [6,10]. Overall, the indicators for Hainan nearshore coral reefs generally fall within the medium to upper range among global coral reef ecosystems, suggesting a certain potential for recovery [7,13,47]. In the future, with the intensification of climate change and human activities, strengthening the dynamic monitoring of foundation species (corals, phytoplankton) and energy flow dynamics will be crucial. This will facilitate the timely identification of trends in ecosystem structural changes and risks of functional degradation, thus providing scientific support for marine ecological management [4,11].

4.2. Regulatory Role of Material Circulation and Key Species Functions

This study revealed that the throughput of each trophic level decreases exponentially with increasing TL, similar to the mass-balance model results of the Xisha coral reef ecosystem [21]. TL I predators accounted for 64.00–89.03% of the total predator consumption, and energy flow to detritus accounted for 67.24–81.70% of the total detrital consumption. This indicated a low energy utilization efficiency at the primary trophic level, where a large amount of energy was stored as detritus at lower trophic levels, making it difficult to transfer upwards. This detritus-dominated material cycling pattern has also been validated in the Nanwan coral reef in Taiwan, where detrital throughput flux is dominant [26]. In the Daya Bay ecosystem, the average transfer efficiency of the overall trophic levels was approximately 10.9% [9], while the corresponding value for the Xisha coral reef system was only 13.15% [21]. The high transfer efficiencies observed in Sanya, Changjiang, and Wenchang suggested a more robust internal energy flow, which may contribute to enhanced system productivity and functional stability. Furthermore, we found that the energy transfer efficiency from detrital food chains in Sanya, Changjiang, and Wenchang was higher than that from primary producers, implying that these three ecosystems were dominated by detrital chains. Conversely, Lingao and Wanning were primarily driven by grazing food chains, a characteristic consistent with the conclusion that primary producers were the main energy source in the Qilianyu coral reef ecosystem [47]. From a functional ecological perspective, research by Bellwood et al. on coral reef resilience indicated that detrital food chains play a crucial role in maintaining ecosystem stability and recovery capabilities by strengthening material and energy recycling [3]. Therefore, this study suggests that in the nearshore coral reef ecosystems of Hainan, the detritus-dominated energy flow pattern not only enhances energy utilization efficiency but might also bolster system resistance to external disturbances.

This study demonstrated that primary producer groups (phytoplankton, reef epilithic turf, and macroalgae) have a significant positive impact on most predators. This finding aligns with observations in the Daya Bay food-web model, where primary and secondary producers exhibited an overall positive effect on mid-to-high trophic level groups, indicating that primary producers in marine areas serve as fundamental hubs for energy and material flow [9]. Regarding the influence of benthic algae on other groups, the MTI values for benthic algae on corals in Sanya and Changjiang were positive, whereas those in Lingao, Wenchang, and Wanning showed a significant negative impact. This regional disparity might be attributed to competition between benthic algae and corals for space, biofilm resources, and differences in nutrient utilization efficiency. This aligns with research on Mexican Caribbean coral reefs, which suggests that high algal cover can weaken the

positive support provided by corals to small fish and invertebrates, subsequently reducing system maturity and stability [6]. Similar phenomena observed in various regions of Hainan suggest that excessive proliferation of benthic algae might already be a potential limiting factor for coral recovery in some areas.

MTI results indicated a general negative impact of fishing on medium and large fish, with the adverse effects being more pronounced in Changjiang, Lingao, Wenchang, and Wanning compared to those in Sanya. This finding is consistent with a trade-off analysis concerning parrotfish catches, which showed that high fishing intensity significantly reduces the maturity of food-web structures and system resilience [44]. Therefore, fishing intensity has been identified as a crucial anthropogenic driver determining the structural health of coral reefs in the South China Sea. High KS and RTI values for functional groups suggested their "keystone" role within the trophic network, exerting a decisive influence on energy flow and network connectivity. This conclusion resonates with an analysis of the Xisha Qilianyu coral reef model, where zooplankton and corals were also identified as the most influential keystone groups within the system, contributing over 50% to system maturity and stability [21]. This aligns with the identification of corals and zooplankton as key functional groups in Sanya in the present study. Furthermore, an investigation into coral health in the Wenchang sea area indicated low coverage of sensitive coral species and high echinoderm biomass, leading to significant fluctuations in health indices, yet possessing recovery potential [13]. This aligns with the identification of corals and echinoderms as key functional groups in Wenchang in the present study. The identification of region-specific keystone groups (e.g., medium carnivorous fish in Wenchang and Wanning) moves beyond general biodiversity protection, allowing for targeted, cost-effective fishery management strategies tailored to each reef's specific structural vulnerability.

4.3. Impacts of Environmental Drivers on Ecological Functions

Oceanic Pic primarily exists as calcium carbonate, with its sources including calcification by marine organisms and the input of terrigenous detritus [48,49]. Additionally, the settling of calcium carbonate shells or skeletons of marine organisms after death also increases the oceanic particulate inorganic carbon content [50]. Ren et al. (2025) observed a significant positive correlation between sediment inorganic carbon content and ecosystem carbon storage in tropical seagrass ecosystems, with this relationship being more pronounced under high-temperature, high-salinity, and coarse sediment conditions [45]. The contributions of terrestrial runoff and marine internal processes to Pic around Hainan coral reefs aligned with the quantitative analysis of local inorganic carbon sources. Pic enhanced carbon fixation by primary producers through increased carbon supply, thereby amplifying energy flow upwards in the system. A proposed Pic threshold (>0.0075 mol/m^2) was introduced as an early-warning level indicating potential ecosystem degradation risk. This threshold was specifically derived from the comparative environmental-response patterns observed in the Ecopath–environmental coupling analysis. At the SEATS station in the South China Sea, the ratio of phytoplankton carbon biomass (C) to Chl_a (C:Chl_a) decreased with depth but remained generally low across all depths [16]. This pattern suggests that Chl_a serves as a crucial indicator for assessing photosynthetic efficiency and the nutritional status of the system. Chl_a ranked second in the comprehensive scoring, indicating the fundamental role of phytoplankton productivity for the primary drivers of coral reefs.

Sea surface temperature exhibited a dual effect on the physiological metabolism of corals and their symbiotic algae: moderate warming can accelerate growth and assimilation, but excessively high temperatures lead to bleaching and a sharp decline in productivity. A simulation study found that under mid-term high-temperature scenarios, the biomass

of corals and large carnivorous fish decreased by 3.8–4.7% in the Xisha Islands [11]. The negative correlation between SST and the total system flux and biomass observed in this study corroborates this finding. The diffuse attenuation coefficient directly regulates the intensity of the underwater light field, which in turn affects the light energy available to photosynthetic organisms. Multiple biogeochemical studies on coral reefs have shown that a lower Kd (i.e., higher water transparency) facilitates the vertical distribution of nutrients and balances photochemical processes, thereby optimizing productivity allocation [3,51]. In this study, although Kd ranked fourth in the importance hierarchy, its local role in energy flow within the seagrass and benthic community module was not negligible.

The functionality and fishery productivity of Hainan nearshore coral reef ecosystems were primarily driven by two carbon source variables: Pic and Chl_a. Sst and Kd modulated the system response through physiological processes and light field regulation, either amplifying or suppressing the effects. This aligned with the combined influence of multiple environmental factors on reef health in Wenchang, Hainan, noting that water quality, thermal conditions, and nutrient levels jointly determine changes in the Coral Health Index [13]. A key practical contribution of this study is the identification of a non-linear peaked relationship between Pic and key ecosystem indicators, yielding an optimal Pic range (0.0050–0.0075 mol/m^2) and an early-warning threshold (>0.0075 mol/m^2). Importantly, the observed non-linear peaked relationship between Pic and ecosystem indicators is unlikely to be an artifact of discrete model inputs. This non-linear pattern is corroborated by cross-ecosystem comparisons [45]. Both seagrass beds and coral reefs rely on carbonate dynamics, suggesting a shared ecological mechanism: moderate Pic levels enhance carbon fixation and primary production, whereas excessive Pic accumulation may lead to physical smothering or alterations in carbonate chemistry that inhibit biological production. This cross-validation supports the robustness of our proposed Pic optimal range (0.0050–0.0075 mol/m^2) as a genuine ecological threshold. Unlike complex dynamic model outputs, this clear environmental threshold can be directly monitored via satellite remote sensing and integrated into existing marine environmental monitoring networks, providing an actionable operational tool for ecosystem managers.

Given the identification of medium carnivorous fish as keystone functional groups in Sanya and Changjiang, and the observed negative impacts of fishing on these groups, precautionary fishing restrictions targeting these species during their potential spawning seasons are recommended, pending future seasonal monitoring data to refine the timing. In contrast, Lingao and Wenchang require more stringent regulation of fishing effort alongside measures to control nutrient inputs, reflecting their reduced trophic transfer efficiency and stronger reliance on detritus-based energy pathways. For Wanning, a combined strategy of adaptive fishery management and habitat restoration is suggested, which is consistent with its intermediate level of ecosystem stability and mixed structural characteristics.

4.4. Limitations of This Research

(1) Sampling design and temporal limitation. Field sampling was conducted during a single dry-season window (February–April 2023). Although this period corresponds to relatively stable monsoon conditions in Hainan, the dataset does not capture seasonal or interannual variability. Therefore, our results represent a synoptic ecological snapshot of reef conditions rather than long-term ecosystem dynamics.

(2) Parameter uncertainty in Ecopath inputs (P/B, Q/B, EE, DC). We explicitly discuss uncertainties associated with all key input parameters, including production/biomass (P/B), consumption/biomass (Q/B), ecotrophic efficiency (EE), and diet composition (DC). These parameters were derived from a combination of field measurements, published literature, FishBase records, and model balancing procedures. We empha-

size that while this is standard practice in EwE applications, it inevitably introduces uncertainty into derived ecosystem indicators.

(3) Absence of full uncertainty propagation (Monte Carlo/bootstrap analysis). A full uncertainty propagation analysis using Monte Carlo simulations or bootstrap methods was not performed because the Ecopath models incorporated heterogeneous parameter sources from multiple functional groups and regions. However, uncertainties associated with major input parameters, including production/biomass (P/B), consumption/biomass (Q/B), ecotrophic efficiency (EE), and diet composition (DC), were considered when interpreting ecosystem indicators. Despite this limitation, the application of a consistent modeling framework, standardized functional-group classification, and identical balancing procedures across regions ensures that the observed spatial patterns remain comparable and robust.

(4) Functional group variability among regions (14–17 groups). We clarify that differences in functional group numbers reflect both real ecological heterogeneity and detectability constraints in field sampling. Ecologically meaningful absences (e.g., low-abundance or habitat-specific taxa) contribute to structural differences among reefs, while acknowledging that rare taxa may also be influenced by sampling limitations. Importantly, all models follow a consistent functional-group framework, ensuring comparability across regions.

(5) Lack of independent validation (e.g., stable isotopes). We explicitly acknowledge that no independent validation dataset (such as stable isotope analysis or tracer-based food-web reconstruction) was available in this study. We recognize this as a limitation of the current work and identify it as a priority for future research to strengthen trophic pathway validation and model calibration.

(6) Limited generalizability of single-year sampling design. The findings presented here represent a spatial comparison of coral reef ecosystem structure and functioning during a specific sampling period rather than a characterization of long-term ecosystem trajectories. Although the standardized sampling design provides a reliable baseline for assessing regional differences under comparable seasonal conditions, temporal variability remains unresolved. Future multi-season and multi-year monitoring efforts are needed to evaluate ecosystem stability, identify long-term trends, and determine whether the observed spatial patterns persist over time. The precise timing of seasonal fishing bans necessitates refinement informed by future seasonal monitoring data. Presently, the recommendations are a precautionary conservation measure, grounded in the identification of key functional groups.

Importantly, despite these limitations, all five Ecopath models were constructed using a consistent methodological framework, standardized functional grouping scheme, and uniform balancing procedure, ensuring that inter-regional comparisons of trophic structure, energy flow, and ecosystem maturity remain internally consistent and methodologically robust. Furthermore, it is important to note that the relationships identified in our GAMs represent correlations based on cross-sectional data from a synoptic survey. While these environmental variables are critical associated factors, long-term manipulative or time-series studies are required to establish definitive causal drivers of ecosystem shifts.

5. Conclusions

This study provides a comparative ecosystem-level assessment of five coral reef systems in Hainan, China, integrating Ecopath food-web modeling with environmental drivers to examine spatial differences in trophic structure, energy flow, and ecosystem organization. By linking ecosystem indicators with environmental gradients and fishing pressure, we developed a framework to interpret how combined anthropogenic and environmental

factors shape reef ecosystem functioning. Overall, the results demonstrate clear spatial heterogeneity among the studied reef systems, with higher trophic complexity and more efficient energy transfer observed in Sanya and Changjiang, while Lingao and Wenchang exhibited simplified trophic structures and stronger reliance on detrital pathways. Wanning showed intermediate characteristics, reflecting a transitional ecosystem state. These patterns collectively highlight strong spatial differentiation in ecosystem maturity across the region. The observed differences in trophic level structure, transfer efficiency, and ecosystem maturity indices are consistent with stronger ecosystem organization under relatively lower fishing pressure, particularly in Sanya and Changjiang. Among multiple environmental variables, particulate inorganic carbon (Pic), chlorophyll-a (Chl_a), and sea surface temperature (Sst) emerged as important correlates of ecosystem structure and energy flow, indicating that both productivity-related and physical forcing factors jointly regulate reef ecosystem functioning. In particular, the response of ecosystem indicators to Pic exhibited a non-linear pattern, suggesting that ecosystem performance may be optimized within a certain environmental range rather than changing linearly across gradients. From a management perspective, these findings emphasize the need for region-specific ecosystem-based strategies. We recommend establishing an early-warning threshold of Pic > 0.0075 mol/m^2 for the Lingao and Wenchang reefs, and implementing seasonal fishing bans in Sanya and Changjiang to protect medium carnivorous fish, which were identified as key groups for maintaining trophic structure. For Wanning, adaptive fishery regulation combined with habitat restoration is suggested to reflect its intermediate ecosystem condition.

Collectively, the results supported all three proposed hypotheses. H1 was supported by the observed spatial differences in trophic structure, energy transfer efficiency, and ecosystem maturity among the five reef regions, with Sanya and Changjiang exhibiting relatively higher trophic complexity and stability. H2 was supported by the identification of particulate inorganic carbon, chlorophyll-a, and sea surface temperature as important environmental correlates regulating ecosystem structure and functioning. H3 was also supported, as fishing pressure showed significant negative effects on medium and large carnivorous fish and influenced regional differences in ecosystem organization and vulnerability. The conclusions of this study are derived from a single-season observational dataset and an Ecopath-based modeling framework, and therefore primarily represent the current spatial patterns of ecosystem structure and functioning across the studied coral reef regions. This comparative assessment provides insights into regional differences in trophic organization and energy flow; however, long-term monitoring and independent validation approaches, such as stable isotope analysis or tracer-based methods, will further improve the resolution of trophic pathways and enhance the assessment of ecosystem dynamics. Overall, this study demonstrates the combined influence of fishing pressure and environmental variability on coral reef ecosystem structure and functioning, and provides a comparative framework to support future ecosystem-based management and conservation planning in tropical reef systems.

Supplementary Materials: The following supporting information can be downloaded at: https://www.mdpi.com/article/10.3390/su18157538/s1, Supplementary file S1: Figures S1–S6; Supplementary file S2: Tables S1–S15.

Author Contributions: J.G., writing—original draft, methodology, investigation, formal analysis; K.C., J.Z., X.L. and G.Z., writing—review and editing, supervision, funding acquisition, conceptualization; L.L., X.H. and D.X., supervision, resources; P.X., writing—review and editing, supervision, methodology, funding acquisition, conceptualization. All authors have read and agreed to the published version of the manuscript.

Funding: This work was supported by funding from the Open Fund of the National Field Scientific Observation and Research Station of Coral Reef Ecosystem in Nansha, Hainan (NSICR24207), Special Project for Basic Scientific Research Business of Central-Level Public Welfare Research Institutes (PM-zx703-202506-155), Guangdong Basic and Applied Basic Research Foundation (2025A1515110157).

Institutional Review Board Statement: The study was a non-experimental field survey of wild fishery resources and did not involve any experimental manipulation, husbandry, or in-laboratory procedures on live animals. Fish and coral specimens were obtained through field sampling around Hainan Island as part of a fishery resource survey carried out in accordance with the fishery laws of the People's Republic of China. No nationally protected or endangered coral and fish species were collected. Under current Chinese legislation, field surveys of wild fishery resources of this kind do not fall within the scope of animal experimentation and do not require approval from an animal ethics committee. For this reason, a formal ethics committee approval is not available.

Informed Consent Statement: Not applicable.

Data Availability Statement: The original contributions presented in this study are included in the article. Further inquiries can be directed to the corresponding author.

Conflicts of Interest: The authors declare no conflicts of interest.

References

1. Ainsworth, C.H.; Mumby, P.J. Coral–algal phase shifts alter fish communities and reduce fisheries production. *Glob. Change Biol.* **2015**, *21*, 165–172. [PubMed]
2. Wang, D.C.; Wu, X.H.; Ding, L.; Zhang, M.S.; Xie, H.; Zhang, Q.; Li, S. Analysis of the Ecosystem Structure and Function of the Yangtze River Estuary Based on the Ecopath Model. *J. Environ. Eng. Technol.* **2022**, *12*, 417–425.
3. Bellwood, D.R.; Hughes, T.P.; Folke, C.; Nyström, M. Confronting the coral reef crisis. *Nature* **2004**, *429*, 827–833. [CrossRef] [PubMed]
4. Alva-Basurto, J.C.; Arias-González, J.E. Modelling the effects of climate change on a Caribbean coral reef food web. *Ecol. Model.* **2014**, *289*, 1–14. [CrossRef]
5. Pauly, D.; Christensen, V.; Walters, C. Ecopath, Ecosim, and Ecospace as tools for evaluating ecosystem impact of fisheries. *ICES J. Mar. Sci.* **2000**, *57*, 697–706. [CrossRef]
6. Argüelles-Jiménez, J.; Alva-Basurto, J.C.; Perez-Espana, H.; Zetina-Rejon, M.J.; Arias-González, J.E. The measurement of ecosystem development in Caribbean coral reefs through topological indices. *Ecol. Ind.* **2020**, *110*, 105866. [CrossRef]
7. Calderon-Aguilera, L.E.; Reyes-Bonilla, H.; Olán-González, M.; Castañeda-Rivero, F.R.; Perusquía-Ardón, J.C. Estimated flows and biomass in a no-take coral reef from the eastern tropical Pacific through network analysis. *Ecol. Ind.* **2021**, *123*, 107359. [CrossRef]
8. Du, J.; Makatipu, P.C.; Tao, L.S.; Pauly, D.; Cheung, W.W.; Peristiwady, T.; Liao, J.; Chen, B. Comparing trophic levels estimated from a tropical marine food web using an ecosystem model and stable isotopes. *Estuar. Coast. Shelf Sci.* **2020**, *233*, 106518. [CrossRef]
9. Chen, Z.; Xu, S.; Qiu, Y. Using a food-web model to assess the trophic structure and energy flows in Daya Bay, China. *Cont. Shelf Res.* **2015**, *111*, 316–326. [CrossRef]
10. Wang, H.Y.; Zhang, X.Y.; Chen, W.L.; Li, Y.C.; Qiu, S.T.; Chen, L.; Du, J.G. Spatial structure and function analysis of Qilianyu multi-habitat marine ecosystem based on Ecospace model. *J. Xiamen Univ.* **2025**, *64*, 433–445.
11. Zhang, X.; Li, Y.; Du, J.; Qiu, S.; Xie, B.; Chen, W.; Wang, J.; Hu, W.; Wu, Z.; Chen, B. Effects of ocean warming and fishing on the coral reef ecosystem: A case study of Xisha Islands, South China Sea. *Front. Mar. Sci.* **2022**, *9*, 1046106. [CrossRef]
12. Capitani, L.; de Araujo, J.N.; Vieira, E.A.; Angelini, R.; Longo, G.O. Ocean warming will reduce standing biomass in a tropical western Atlantic reef ecosystem. *Ecosystems* **2022**, *25*, 843–857.
13. Lang, S.K.; Pang, Q.Z.; Luo, L.Z.; Xu, B.X.; Zhang, J.; Li, Y.C. Description of health status of coral reef ecosystem of Wenchang, Hainan and analysis of its influencing factors. *Trans. Oceanol. Limnol.* **2024**, *46*, 80–88.
14. *GB/T 12763.9*; Specifications for Oceanographic Survey—Part 9: Guidelines for Marine Ecological Survey. China Standards Press: Beijing, China, 2007.
15. Brown, P.C.; Painting, S.J.; Cochrane, K.L. Estimates of phytoplankton and bacterial biomass and production in the northern and southern Benguela ecosystems. *S. Afr. J. Mar. Sci.* **1991**, *11*, 537–564. [CrossRef]
16. Shang, Y.W.; Xiao, W.P.; Liu, X. Variations of pico-phytoplankton groups and carbon to chlorophyll-a ratios in the South China Sea at the SEATS station. *J. Xiamen Univ.* **2018**, *57*, 811–818.

17. Ke, Z.; Tan, Y.; Huang, L.; Liu, H.; Liu, J.; Jiang, X.; Wang, J. Spatial distribution patterns of phytoplankton biomass and primary productivity in six coral atolls in the central South China Sea. *Coral Reefs* **2018**, *37*, 919–927. [CrossRef]
18. Wabnitz, C.; Balazs, G.; Beavers, S.; Bjorndal, K.; Bolten, A.; Christensen, V.; Hargrove, S.; Pauly, D. Ecosystem structure and processes at Kaloko Honokōhau, focusing on the role of herbivores, including the green sea turtle Chelonia mydas, in reef resilience. *Mar. Ecol. Prog. Ser.* **2010**, *420*, 27–44. [CrossRef]
19. Cáceres, I.; Ortiz, M.; Cupul-Magaña, A.L.; Rodríguez-Zaragoza, F.A. Trophic models and short-term simulations for the coral reefs of Cayos Cochinos and Media Luna (Honduras): A comparative network analysis, ecosystem development, resilience, and fishery. *Hydrobiologia* **2016**, *770*, 209–224.
20. Ruiz, D.J.; Banks, S.; Wolff, M. Elucidating fishing effects in a large-predator dominated system: The case of Darwin and Wolf Islands (Galápagos). *J. Sea Res.* **2016**, *107*, 1–11. [CrossRef]
21. Hong, X.; Chen, Z.; Zhang, J.; Jiang, Y.E.; Gong, Y.; Cai, Y.; Yang, Y. Construction and analysis of a coral reef trophic network for Qilianyu Islands, Xisha Islands. *Acta Oceanol. Sin.* **2022**, *41*, 58–72. [CrossRef]
22. Xu, P.; Huang, L.T.; Zhang, Y.Y.; Huang, H. Different degrees of decline in China's ffshing efforts are beneficial to the sustainable development of coral reef fisheries resources on Yongxing Island China. *Ecol. Model.* **2024**, *494*, 110766. [CrossRef]
23. Du, F.Y.; Wang, X.H.; Lin, Z.J. The characteristics of summer zooplankton community in the Meiji coral reef, Nansha Islands, South China Sea. *Acta Ecol. Sin.* **2015**, *35*, 1014–1021. [CrossRef]
24. Allen, K.R. Relation between production and biomass. *J. Fish. Board Can.* **1971**, *28*, 1573–1581. [CrossRef]
25. Palomares, M.L.D.; Pauly, D. Predicting food consumption of fish populations as functions of mortality, food type, morphometrics, temperature and salinity. *Mar. Freshw. Res.* **1998**, *49*, 447–453. [CrossRef]
26. Liu, P.-J.; Shao, K.-T.; Jan, R.-Q.; Fan, T.-Y.; Wong, S.-L.; Hwang, J.-S.; Chen, J.-P.; Chen, C.-C.; Lin, H.-J. A trophic model of fringing coral reefs in Nanwan Bay, southern Taiwan suggests overfishing. *Mar. Environ. Res.* **2009**, *68*, 106–117. [CrossRef] [PubMed]
27. Bozec, Y.M.; Gascuel, D.; Kulbicki, M. Trophic model of lagoonal communities in a large open atoll (Uvea, Loyalty islands, New Caledonia). *Aquat. Living Resour.* **2004**, *17*, 151–162. [CrossRef]
28. Gaither, M.R.; Bowen, B.W.; Bordenave, T.-R.; A Rocha, L.; Newman, S.J.; A Gomez, J.; van Herwerden, L.; Craig, M.T. Phylogeography of the reef fish *Cephalopholis argus* (Epinephelidae) indicates Pleistocene isolation across the Indo-Pacific Barrier with contemporary overlap in the Coral Triangle. *BMC Evol. Biol.* **2011**, *11*, 189. [CrossRef] [PubMed]
29. Christensen, V.; Walters, C.J.; Pauly, D. *Ecopath with Ecosim: A User's Guide*; Fisheries Centre University of British Columbia: Vancouver, BC, Canada, 2005; 154p.
30. Walters, C.; Martell, S.J.; Christensen, V.; Mahmoudi, B. An Ecosim model for exploring Gulf of Mexico ecosystem management options: Implications of including multistanza life-history models for policy predictions. *Bull. Mar. Sci.* **2008**, *83*, 251–271.
31. Li, Y.; Chen, Z.; Zhang, J.; Jiang, Y.; Gong, Y.; Cai, Y.; Yang, Y.T. Species and taxonomic diversity of Qilianyu island reef fish in the Xisha Islands. *J. Fish. Sci. China* **2020**, *27*, 815–823.
32. Hainan Provincial Bureau of Statistics. *Hainan Statistical Yearbook*; China Statistics Press: Beijing, China, 2019.
33. Hainan Provincial Bureau of Statistics. *Hainan Statistical Yearbook*; China Statistics Press: Beijing, China, 2023.
34. Link, J.S. Adding rigor to ecological network models by evaluating a set of pre-balance diagnostics: A plea for PREBAL. *Ecol. Model.* **2010**, *221*, 1580–1591. [CrossRef]
35. Heymans, J.J.; Coll, M.; Link, J.S.; Mackinson, S.; Steenbeek, J.; Walters, C.; Christensen, V. Best practice in Ecopath with Ecosim food-web models for ecosystem-based management. *Ecol. Model.* **2016**, *331*, 173–184. [CrossRef]
36. Steel, E.A.; McElhany, P.; Yoder, N.J.; Purser, M.D.; Malone, K.; Thompson, B.E.; Avery, K.A.; Jensen, D.; Blair, G.; Busack, C.; et al. Making the best use of modeled data: Multiple approaches to sensitivity analysis of a fish-habitat model. *Fisheries* **2009**, *34*, 330–339. [CrossRef]
37. Ulanowicz, R.E.; Puccia, C.J. Mixed trophic impacts in ecosystems. *Coenoses* **1990**, *5*, 7–16.
38. Libralato, S.; Christensen, V.; Pauly, D. A method for identifying keystone species in food web models. *Ecol. Model.* **2006**, *195*, 153–171. [CrossRef]
39. Finn, J.T. Measures of ecosystem structure and function derived from analysis of flows. *J. Theor. Biol.* **1976**, *56*, 363–380. [CrossRef] [PubMed]
40. Ortiz, M.; Berrios, F.; Campos, L.; Uribe, R.; Ramirez, A.; Hermosillo-Núñez, B.; González, J.; Rodriguez-Zaragoza, F. Mass balanced trophic models and short-term dynamical simulations for benthic ecological systems of Mejillones and Antofagasta bays (SE Pacific): Comparative network structure and assessment of human impacts. *Ecol. Model.* **2015**, *309*, 153–162. [CrossRef]
41. Odum, E.P. The Strategy of Ecosystem Development: An understanding of ecological succession provides a basis for resolving man's conflict with nature. *Science* **1969**, *164*, 262–270. [CrossRef] [PubMed]
42. Landi, P.; Minoarivelo, H.O.; Brännström, Å.; Hui, C.; Dieckmann, U. Complexity and stability of ecological networks: A review of the theory. *Popul. Ecol.* **2018**, *60*, 319–345. [CrossRef]
43. Heymans, S. Comparing the Newfoundland marine ecosystem models using information theory. *Fish. Cent. Res. Rep.* **2003**, *11*, 62–71.

44. Bozec, Y.M.; O'Farrell, S.; Bruggemann, J.H.; Luckhurst, B.E.; Mumby, P.J. Tradeoffs between fisheries harvest and the resilience of coral reefs. *Proc. Natl. Acad. Sci. USA* **2016**, *113*, 4536–4541. [CrossRef]
45. Ren, Y.; Liu, S.; Liang, J.; Akhand, A.; Luo, H.; Jiang, Z.; Wu, Y.; Huang, X.; Macreadie, P.I. Improving Carbon Budgets by Accounting for Inorganic Carbon in Seagrass Ecosystems. *Glob. Change Biol.* **2025**, *31*, e70060. [CrossRef] [PubMed]
46. Pint, S.; Stevens, M.; Musimwa, R.; Standaert, W.; De Troch, M.; van Oevelen, D.; Heymans, J.J.; Everaert, G. A food web model of the Southern Bight of the North Sea. *Ocean Coast. Manag.* **2024**, *255*, 107256. [CrossRef]
47. Hong, X.F.; Chen, Z.Z.; Zhang, J.; Jiang, Y.E.; Gong, Y.Y.; Cai, Y.C.; Yang, Y.T. Analysis of ecological carrying capacity of reef organisms in Qilianyu Islands based on Ecopath model. *J. Trop. Ocean.* **2022**, *41*, 15–27. [CrossRef]
48. Millero, F.J. The marine inorganic carbon cycle. *Chem. Rev.* **2007**, *107*, 308–341. [CrossRef] [PubMed]
49. Müller, G.; Börker, J.; Sluijs, A.; Middelburg, J.J. Detrital carbonate minerals in Earth's element cycles. *Glob. Biogeochem. Cycles* **2022**, *36*, e2021GB007231. [CrossRef]
50. Toullec, J. Evaluation of the Particulate Inorganic Carbon Export Efficiency in the Global Ocean. *Biogeosciences* **2026**, *23*, 4361–4377. [CrossRef]
51. Sert, M.F.; Bernstein, H.C.; Dølven, K.O.; Petters, S.; Kekäläinen, T.; Jänis, J.; Corrales-Guerrero, J.; Ferré, B. Cold seeps and coral reefs in Northern Norway: Carbon cycling in marine ecosystems with coexisting features. *J. Geophys. Res. Biogeo.* **2025**, *130*, e2024JG008475. [CrossRef]